

Key points from Week 1...

Hydrostatic vs. nonhydrostatic phenomena

Development of buoyancy, usage of virtual temperature ($T_v = T(1 + 0.61q)$; $q = \frac{1+w}{w}$)

Parcel Theory using simplified vertical momentum equation ($\frac{dw}{dt} = B \cong \frac{T'_v}{\bar{T}_v} = \frac{\theta'_v}{\theta_v}$)

CAPE and CIN definitions

Maximum updraft speed “thermodynamic speed limit” ($w_{max} = \sqrt{2 * CAPE}$)

Use of skew-T to determine buoyancy and resulting vertical motions

Limitations of parcel theory ($dw/dt = B$)

1. Entrainment (parcel theory assumes no interaction between parcel and environment)
2. Hydrometeor effects (parcel theory assumes no hydrometeors present)
 1. Loading (drag; reduces accelerations from buoyancy alone)
 2. Warming
 3. Freezing
3. Environmental subsidence (parcel theory assumes constant env)
4. Pressure perturbations (neglected *twice* - impact on buoyancy and in dp'/dz term in vertical momentum equation)

Anelastic and Boussinesq equation sets

Equation sets (momentum, continuity, etc.) allow for buoyancy, simplify other dynamics

1) Anelastic assumption

- removes “slackness” of air ($c = \infty$)
- density only a function of height, unless associated with buoyancy
- pressure NOT independent, it is a diagnostic variable, dependent on wind & buoyancy
- pressure perturbations “felt” by every other point in domain simultaneously (cant determine pressure perturbation only at one point, have to solve it everywhere at once).
- appropriate when $u^2 \ll c^2$

2) Boussinesq assumption

- atmosphere is incompressible, constant density, unless associated with buoyancy
- same restrictions as above involving pressure
- appropriate when $D \ll H$ (~ 8 km)

Forms of mass conservation equations

Equation sets (momentum, continuity, etc.) allow for buoyancy, simplify other dynamics

$$\frac{d\rho}{dt} + \rho (\nabla \cdot \mathbf{v}) = 0.$$

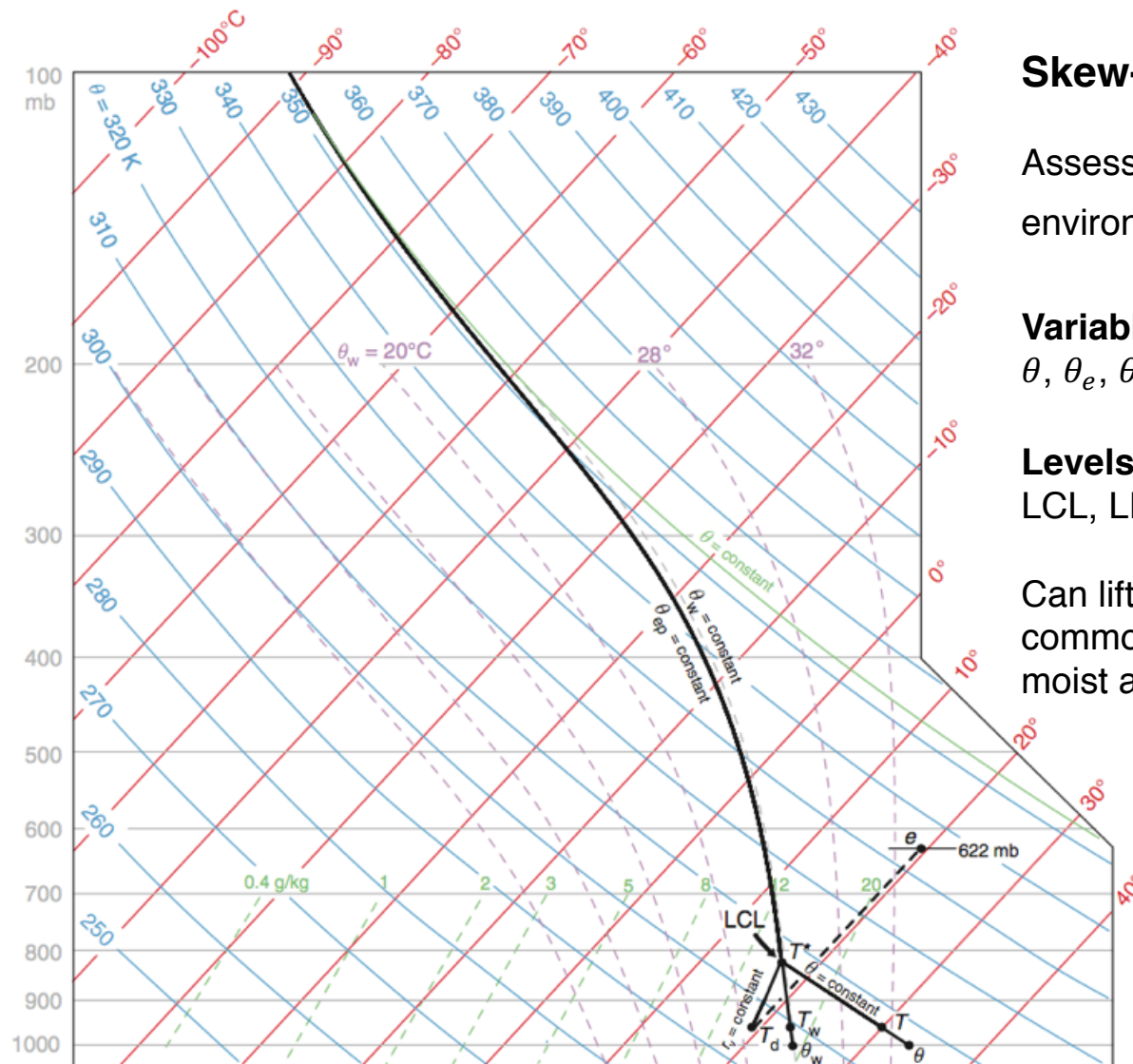
Full mass continuity, Lagrangian view

$$\nabla \cdot (\rho_a \mathbf{v}) = 0,$$

Anelastic mass continuity

$$\nabla \cdot \mathbf{v} = 0,$$

Boussinesq mass continuity
(incompressible form)



Skew-T Diagram Review

Assess differences between lifted parcel and environment ($B \cong \frac{T'_V}{\bar{T}_V}$; integrated B = CAPE)

Variables:

$\theta, \theta_e, \theta_v, \theta_w, \theta_\rho$

Levels:

LCL, LFC, EL

Can lift parcel from anywhere! Most commonly the surface. Always follow dry or moist adiabats.

Reversible vs. Pseudoadiabatic lapse rates

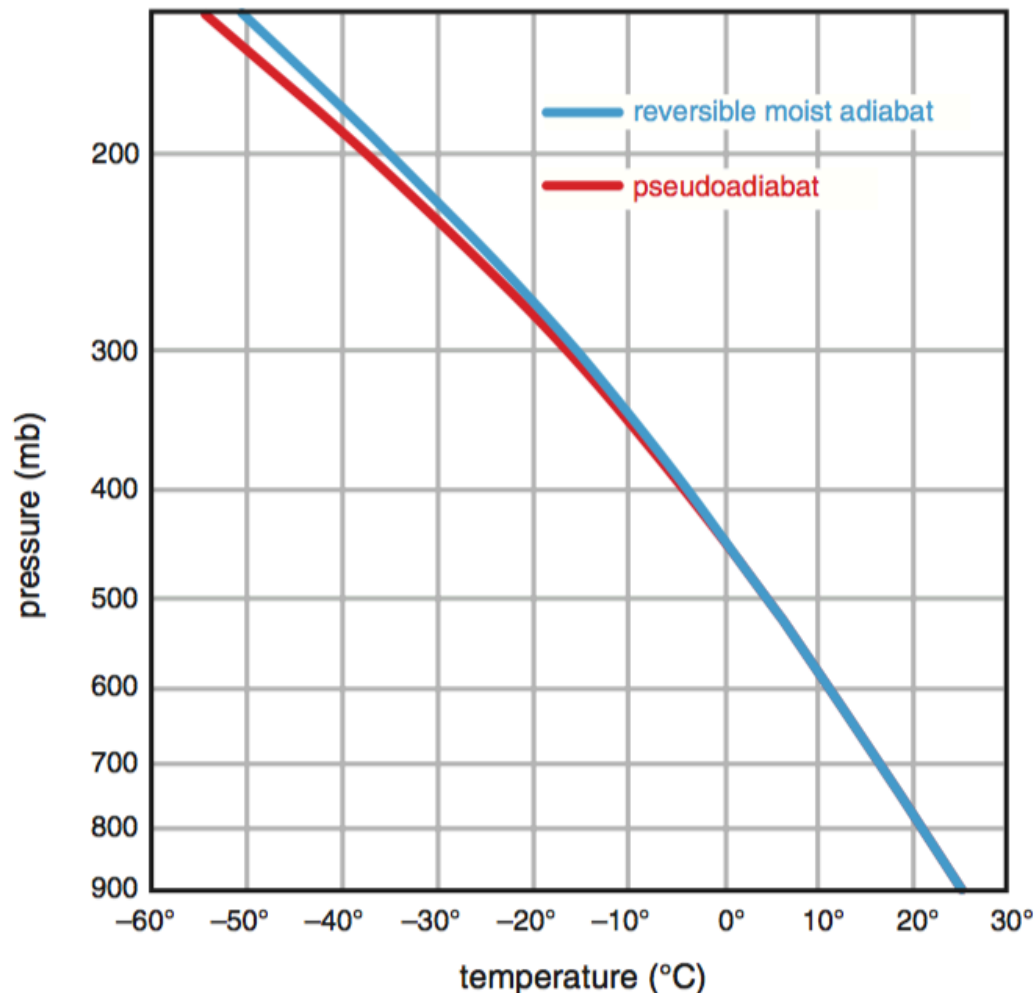
Reversible – condensate stays with parcel
Latent heating absorbed by gaseous portion AND hydrometeors (θ_e)

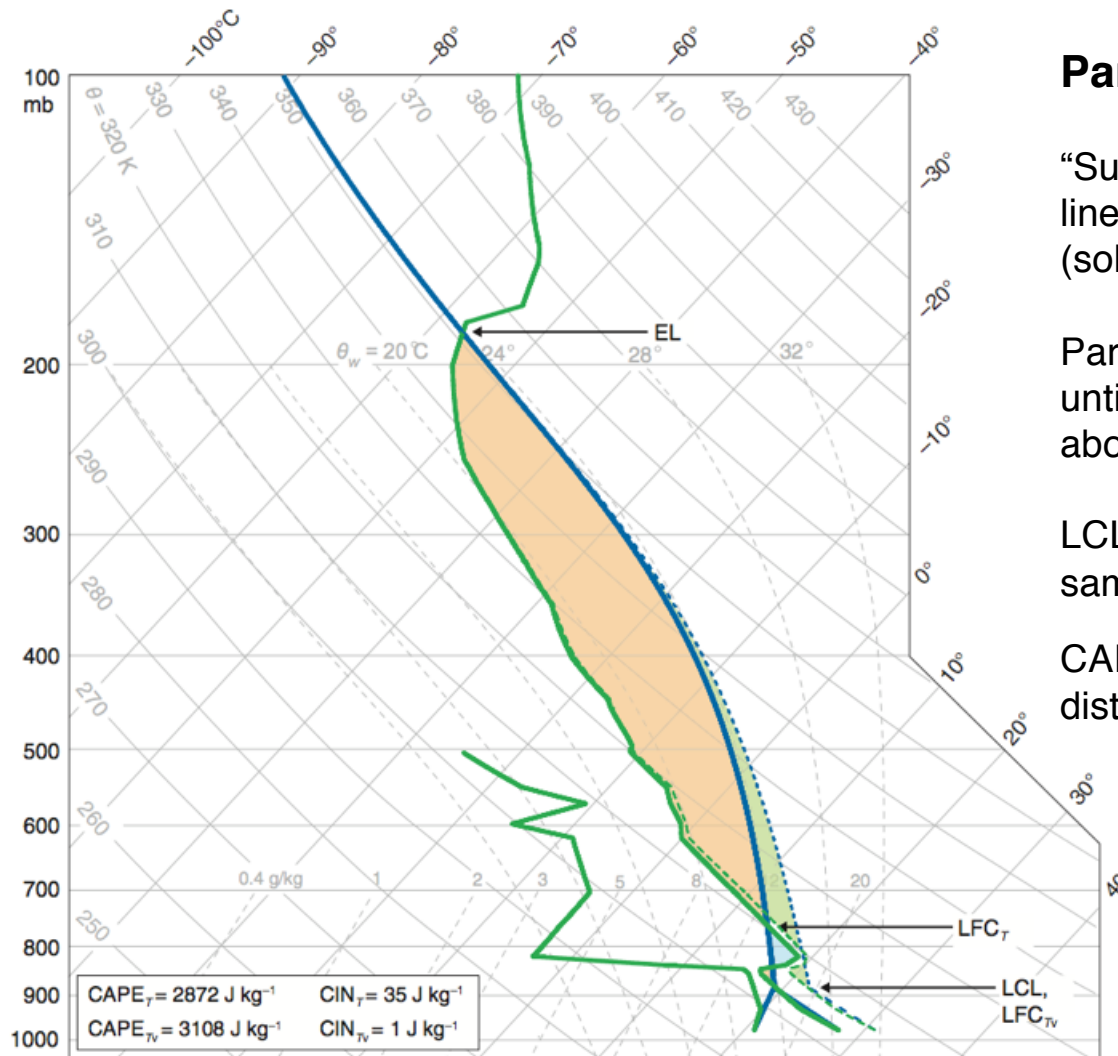
Pseudoadiabatic – condensate ignored
Latent heating absorbed by only gaseous portion of parcel (θ_{ep})

Largest difference aloft – impact of heat content of hydrometeors rising with parcel

Skew-T uses pseudoadiabatic ascent lines

Real atmospheric processes are between these two extremes





Parcel Theory on Skew-T

“Surface-based” convection example. Blue lines – parcel, green lines - environment (solid= T , dashed= T_v).

Parcel lifted from surface, follows DALR until LCL (mixing ratio conserved), MALR above LCL. CAPE/CIN shaded.

LCL *same* if using T or T_v – LFC is *not* the same.

CAPE sometimes normalized by depth (to distinguish between CAPE profiles).

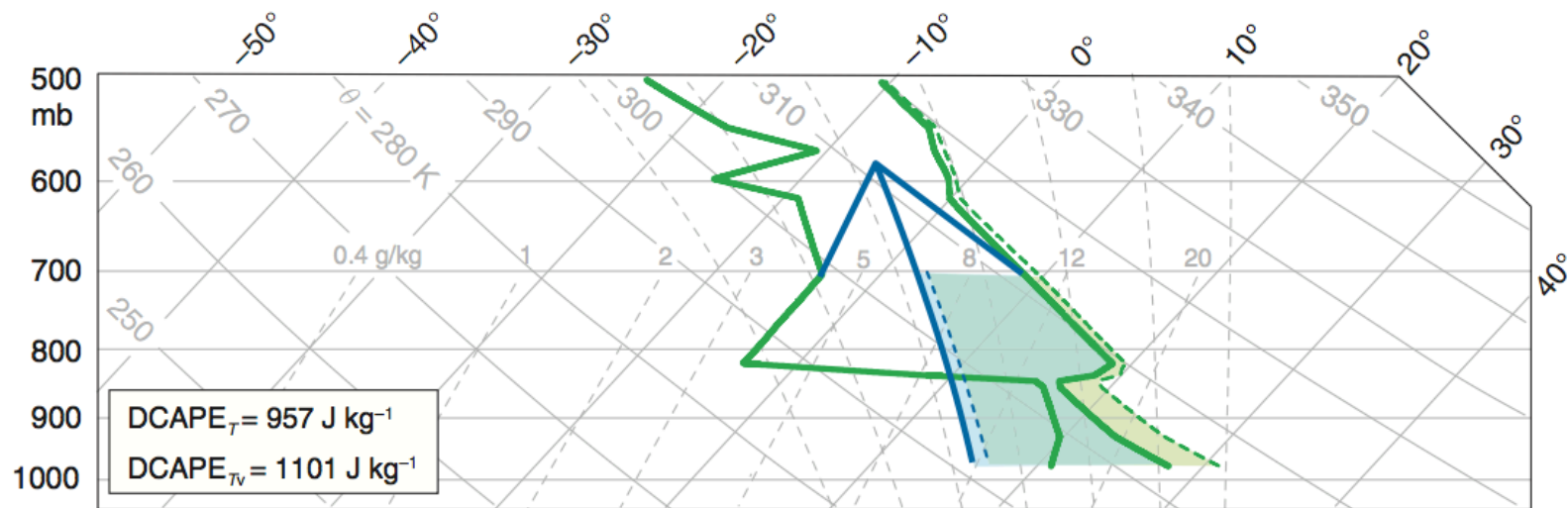
$$\text{CAPE} = \int_{\text{LFC}}^{\text{EL}} B \, dz \approx g \int_{\text{LFC}}^{\text{EL}} \frac{T'_v}{\bar{T}_v} \, dz$$

$$\text{CIN} = - \int_0^{\text{LFC}} B \, dz \approx -g \int_{\text{SFC}}^{\text{LFC}} \frac{T'_v}{\bar{T}_v} \, dz$$

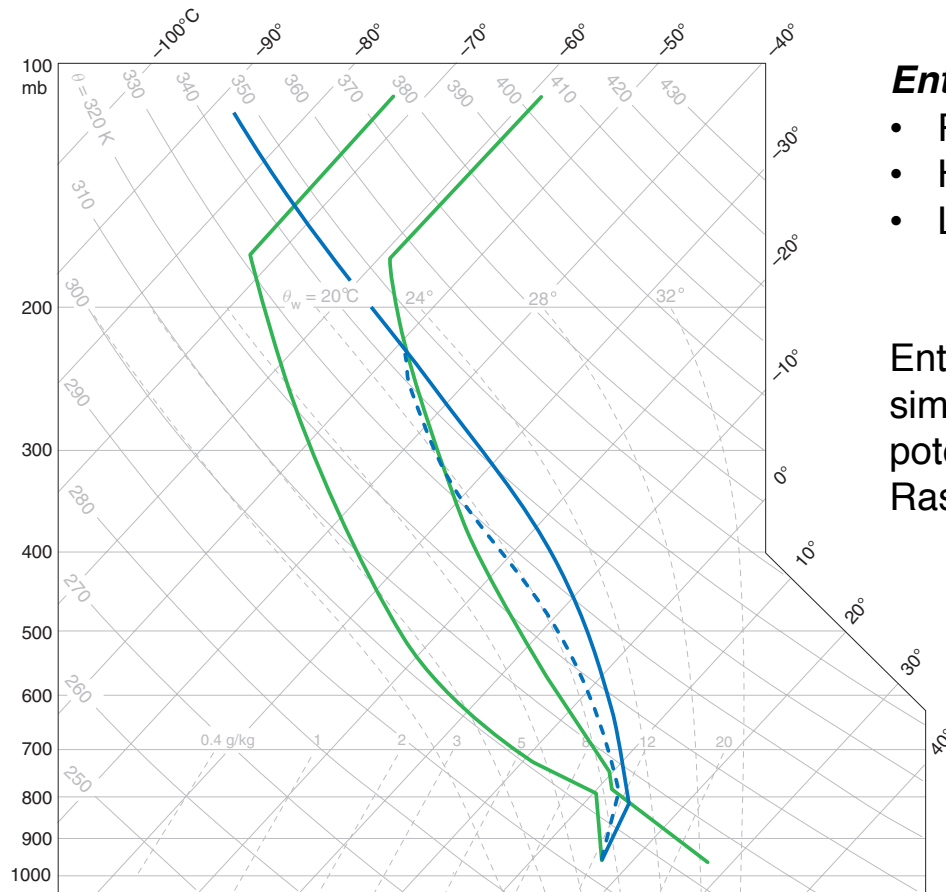
Parcel Theory on Skew-T

DCAPE: Downdraft CAPE – used to estimate potential strength (i.e., w) of evaporatively-cooled downdrafts. Where to start is not obvious, and parcels could become unsaturated. Parcel with lowest θ_e useful for minimum cold pool temperature.

$$\text{DCAPE} = g \int_h^0 \frac{T'_v}{\bar{T}_v} dz,$$



More on entrainment...



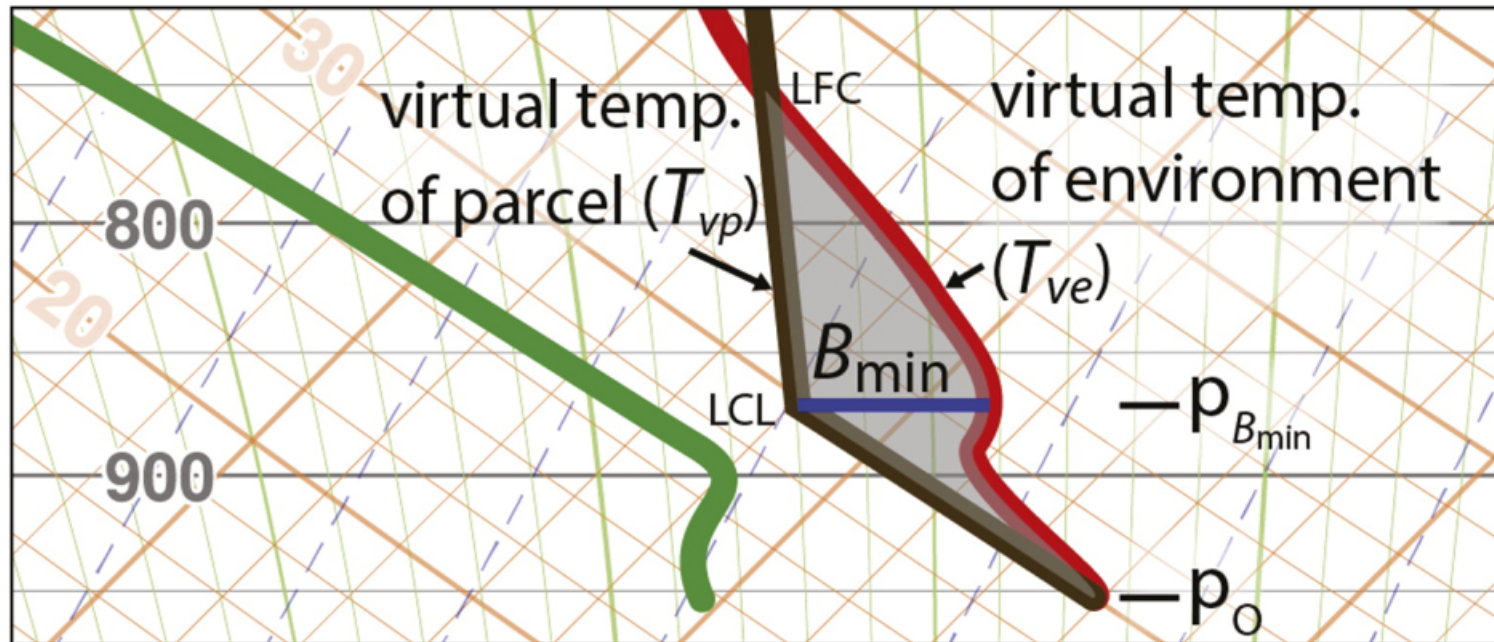
Entrainment effects:

- Reduced CAPE
- Higher cloud base
- Lower cloud top

Entrainment rates not well established. High-resolution simulations suggest rates up to 10% per kilometer, potentially reducing CAPE up to 50% (Ziegler and Rasmussen 1998; Trier et al. 2014).

Solid blue – undilute parcel (no entrainment)
Dashed blue – dilute parcel (with entrainment)
Green – environmental profile

Level of minimum buoyancy: related to CIN (Trier et al. 2014)

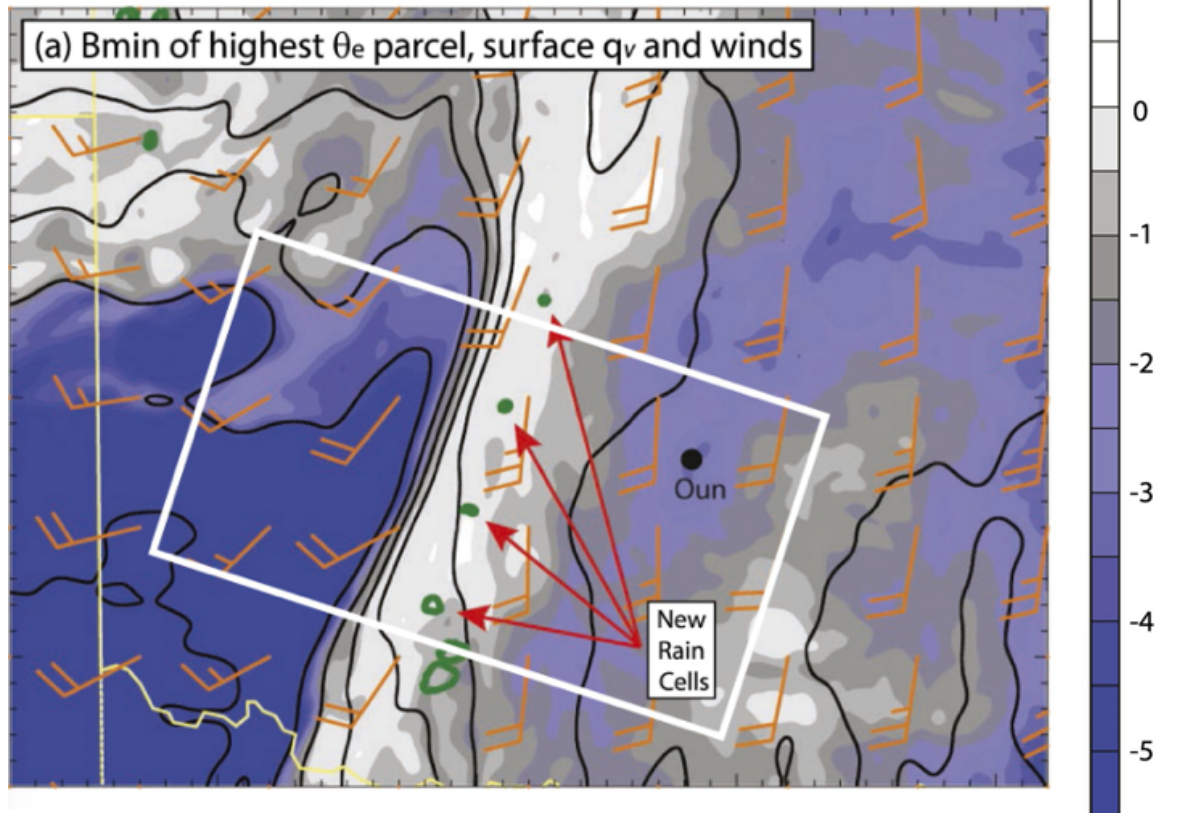


Shaded area = CIN

$P_{B_{min}}$ – pressure level of minimum buoyancy

Level of minimum buoyancy: related to CIN (Trier et al. 2014)

Ensemble Member 6 in D03 ($\Delta = 1$ km) at 1900 UTC (t = 4h)



Oklahoma 2013 Tornado Outbreak Skew-T

“**SB**” parcel – use surface T / w

“**ML**” parcel – use mean T / w in lowest 100 mb
“mixed-layer”.

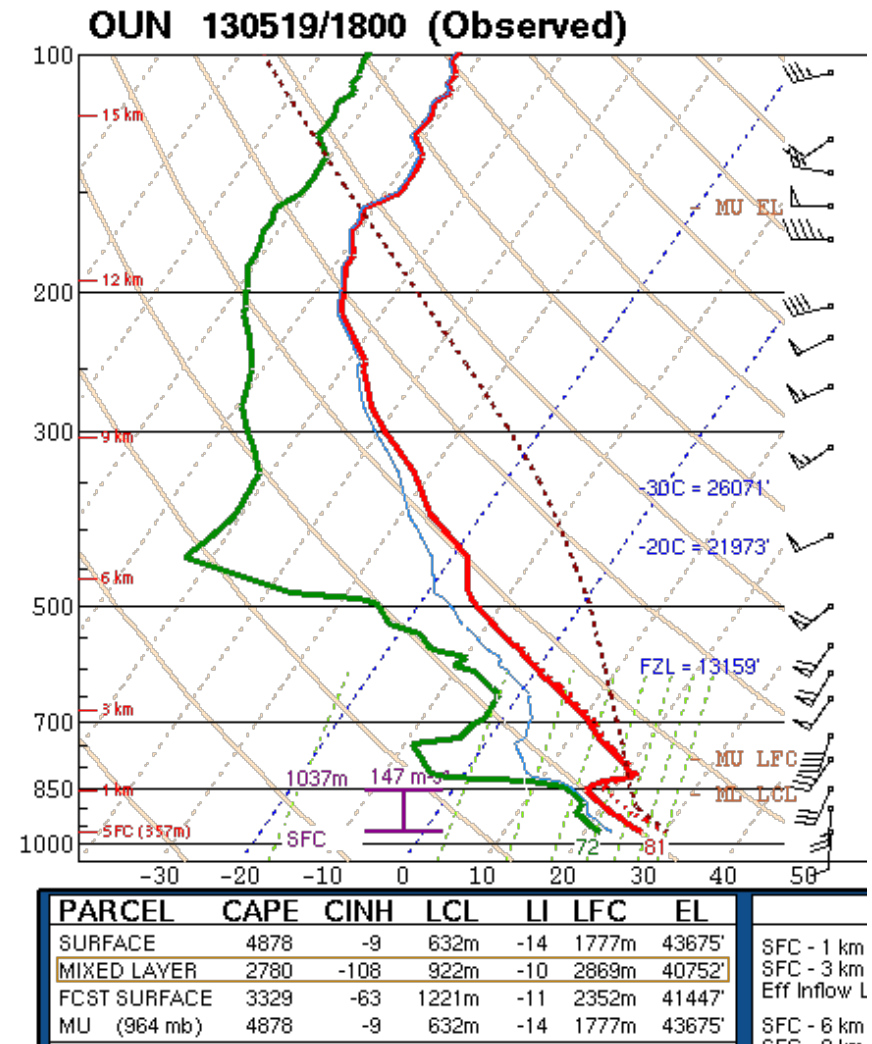
“**MU**” parcel – use highest θ_e found in lowest 300 mb.
“most unstable, largest CAPE”

Parcel type has impact on CAPE/CIN values.

Virtual temperature impacts...

Large CIN with surface parcel using T.

Almost no CIN for surface parcel using T_v .



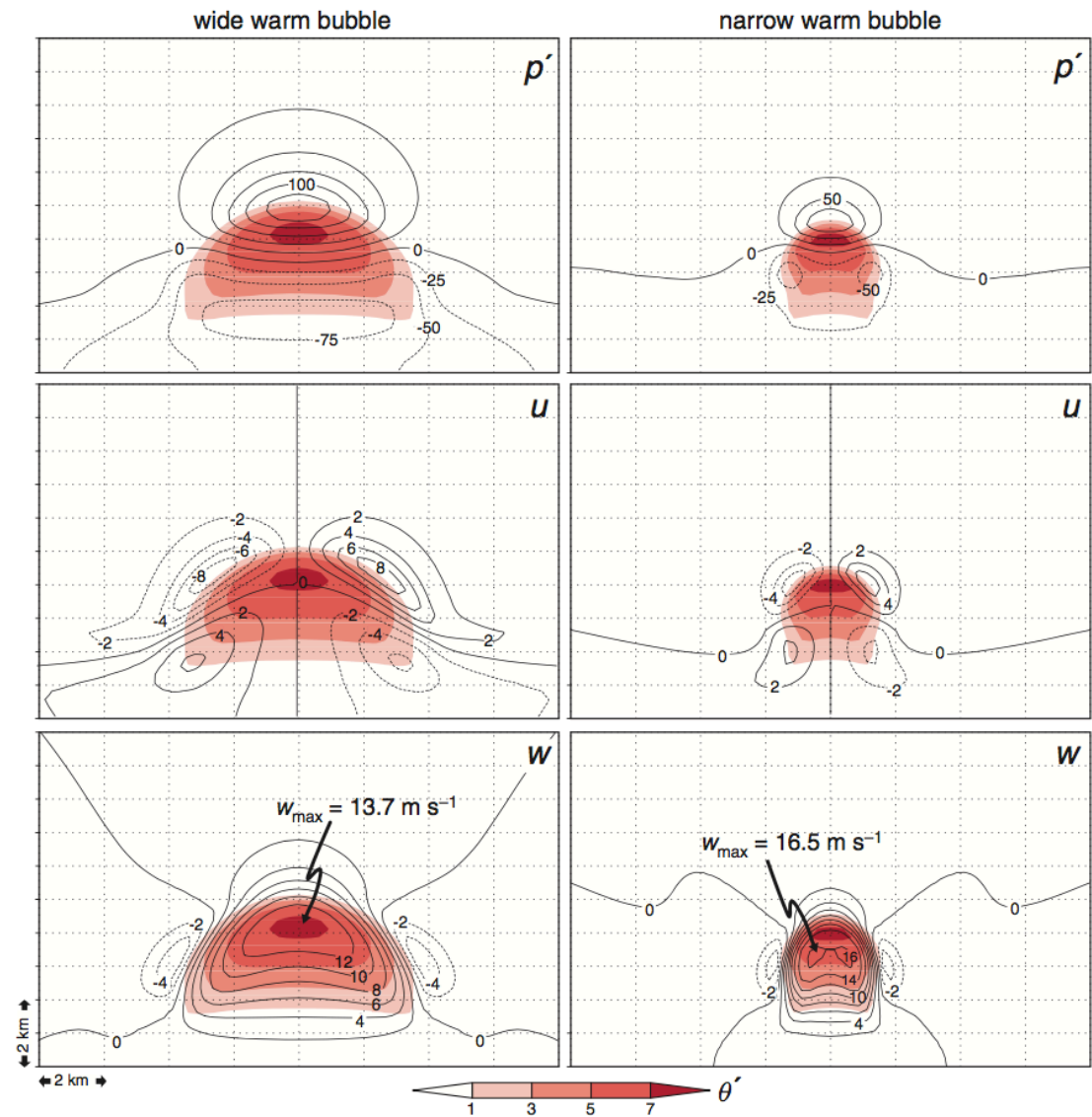
Effects of VPPGF

Neglected in parcel theory.

In this case, VPPGF acts in opposite direction of buoyancy.

As bubble (parcel) width increases, the VPPGF increases, but buoyancy remains the same.

Resultant vertical velocity within parcel is reduced as width increases.



The origins of pressure perturbations (MR 2.5)

- pressure perturbations may arise from density anomalies or from wind speed gradients, and perturbation pressure *gradients* may, in turn, influence the wind in important ways
 - reduction of vertical velocity (generally the case)
 - enhancement of vertical velocity in some special cases (may intensify storms or rotation within storms)
 - forced lifting of air to the LFC (critical to storm maintenance and propagation)
- nonhydrostatic vs hydrostatic pressure
- dynamic vs buoyancy pressure



The origins of pressure perturbations

Describe the pressure and density as the sum of a horizontally homogeneous base state pressure and density, respectively, and a deviation from this base state, i.e.,

$$p(x, y, z, t) = \bar{p}(z) + p'(x, y, z, t)$$

$$\rho(x, y, z, t) = \bar{\rho}(z) + \rho'(x, y, z, t)$$

The base state is in hydrostatic balance, i.e.,

$$0 = -\frac{\partial \bar{p}}{\partial z} - \bar{\rho}g$$

The inviscid vertical momentum equation then can be written as

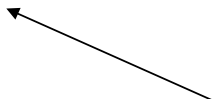
$$\frac{dw}{dt} = -\frac{1}{\rho} \frac{\partial p'}{\partial z} - \frac{\rho'}{\rho} g$$

Hydrostatic and nonhydrostatic pressure perturbations

We can represent the perturbation pressure as the sum of a hydrostatic pressure perturbation (p'_h) and a nonhydrostatic pressure perturbation (p'_{nh}), i.e.,

$$p' = p'_{nh} + p'_h$$

arises from density perturbations
by way of the relation $\frac{\partial p'_h}{\partial z} = -\rho'g$

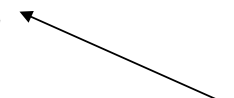


Thus we can rewrite the vertical momentum equation as

$$\frac{dw}{dt} = -\frac{1}{\rho} \frac{\partial p'_{nh}}{\partial z} \quad \text{Vertical acceleration results from non-hydrostatic pressure perturbations.}$$

Hydrostatic pressure perturbations

$$p' = p'_{nh} + p'_h$$


 arises from density perturbations
by way of the relation $\frac{\partial p'_h}{\partial z} = -\rho'g$

After integrating hydrostatic equation...

$$\frac{\partial p}{\partial t} = -g \int_z^\infty \left[\frac{\partial(\rho u)}{\partial x} + \frac{\partial(\rho v)}{\partial y} \right] dz + g\rho w$$

Hydrostatic pressure is the “weight” of atmosphere above a point.

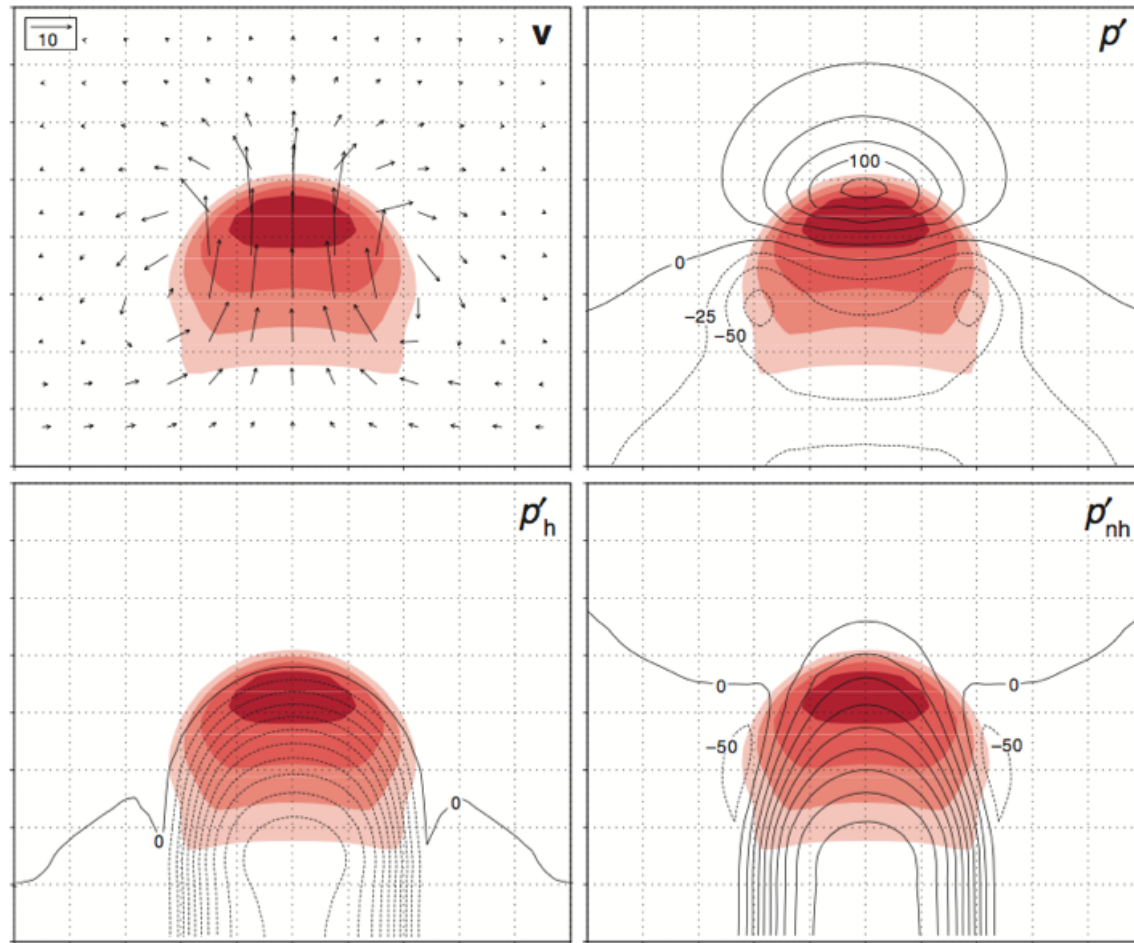
Hydrostatic pressure changes at a height, z , are due to changes in the “weight” of the atmosphere above height z .

Weight changes due to more/less mass above a point:

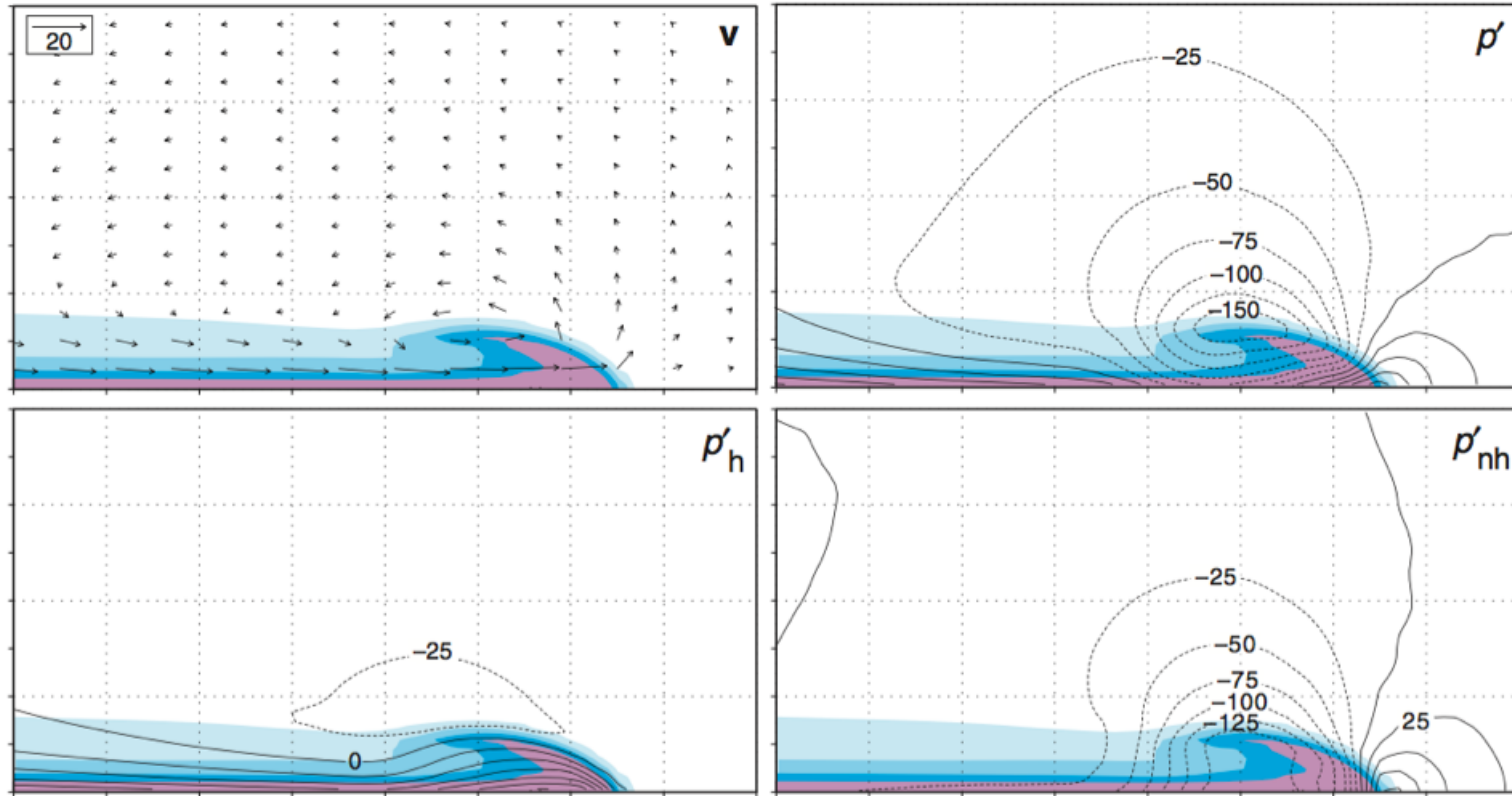
- net mass divergence/convergence above point (term 1 on RHS)
- vertical advection of mass into column from below (term 2 on RHS; if $w=0$, this term vanishes).

Accomplished through warm/cold advection, rising/sinking motion, diabatic heating (using hypsometric eqn).

Hydrostatic pressure perturbation associated with positively buoyant bubble



Hydrostatic pressure perturbation associated with density current



Dynamic and buoyancy pressure perturbations

Another common approach undertaken to decompose the perturbation pressure is to form a diagnostic pressure equation by taking the divergence of the three-dimensional **Boussinesq** momentum equation,

$$\nabla \cdot \left[\frac{\partial \mathbf{v}}{\partial t} + \mathbf{v} \cdot \nabla \mathbf{v} = -\alpha_o \nabla p' + B\mathbf{k} - f\mathbf{k} \times \mathbf{v} \right]$$

Where $\mathbf{v} = (u, v, w)$ is the velocity vector, $\alpha_o \equiv 1/\rho_o$ is a constant specific volume, and f is the Coriolis parameter (the Coriolis force has been approximated as $-f\mathbf{k} \times \mathbf{v}$).

Dynamic and buoyancy pressure perturbations

$$\nabla^2 f = \nabla \cdot \nabla f$$

Thus, we have

Laplacian = divergence of gradient of f

$$\frac{\partial(\nabla \cdot \mathbf{v})}{\partial t} + \nabla \cdot (\mathbf{v} \cdot \nabla \mathbf{v}) = -\alpha_o \nabla^2 p' + \frac{\partial B}{\partial z} - \nabla \cdot (f \mathbf{k} \times \mathbf{v})$$

Using $\nabla \cdot \mathbf{v} = 0$, we obtain

$$\alpha_o \nabla^2 p' = -\nabla \cdot (\mathbf{v} \cdot \nabla \mathbf{v}) + \frac{\partial B}{\partial z} - \nabla \cdot (f \mathbf{k} \times \mathbf{v})$$

And after evaluating $\nabla \cdot (\mathbf{v} \cdot \nabla \mathbf{v})$ and $\nabla \cdot (f \mathbf{k} \times \mathbf{v})$, we obtain

$$\begin{aligned} \alpha_o \nabla^2 p' = & - \left[\left(\frac{\partial u}{\partial x} \right)^2 + \left(\frac{\partial v}{\partial y} \right)^2 + \left(\frac{\partial w}{\partial z} \right)^2 \right] \\ & - 2 \left(\frac{\partial v}{\partial x} \frac{\partial u}{\partial y} + \frac{\partial w}{\partial x} \frac{\partial u}{\partial z} + \frac{\partial w}{\partial y} \frac{\partial v}{\partial z} \right) + \frac{\partial B}{\partial z} + f\zeta - \beta u \end{aligned}$$

$\zeta = \frac{\partial v}{\partial x} - \frac{\partial u}{\partial y}$
 $\beta = df/dy$

Dynamic and buoyancy pressure perturbations

$$\alpha_o \nabla^2 p' = - \left[\left(\frac{\partial u}{\partial x} \right)^2 + \left(\frac{\partial v}{\partial y} \right)^2 + \left(\frac{\partial w}{\partial z} \right)^2 \right] \quad \text{relatively unimportant on convective scales}$$

$$-2 \left(\frac{\partial v}{\partial x} \frac{\partial u}{\partial y} + \frac{\partial w}{\partial x} \frac{\partial u}{\partial z} + \frac{\partial w}{\partial y} \frac{\partial v}{\partial z} \right) + \frac{\partial B}{\partial z} + \cancel{f\zeta} - \cancel{\beta u}$$

dominates on the synoptic scale

very small on all scales

$$\therefore \alpha_o \nabla^2 p' = f\zeta$$

when p' is reasonably “well-behaved,”

Laplacian of wavelike variable tends to be

positive where perturbations are negative, and vice versa...

$$\nabla^2 p' \propto -p' \longrightarrow p' \propto -f\zeta$$

Synoptic-scale
cyclones/anticyclones

Dynamic and buoyancy pressure perturbations

In M&R, first set of terms on RHS combined into "splat" and "spin" terms using rate-of-strain tensor, e_{ij} ,

$$e_{ij}^2 = \frac{1}{4} \sum_{i=1}^3 \sum_{j=1}^3 \left(\frac{\partial u_i}{\partial x_j} + \frac{\partial u_j}{\partial x_i} \right)^2$$

where $u_1=u$, $u_2=v$, $u_3=w$, $x_1=x$, $x_2=y$, $x_3=z$

magnitude of vorticity vector ($\nabla \times \mathbf{v}$)

$$p' \propto \underbrace{\underbrace{e_{ij}^2}_{\text{splat}} - \underbrace{\frac{1}{2}|\boldsymbol{\omega}|^2}_{\text{spin}}}_{\text{dynamic pressure perturbation}} \underbrace{- \frac{\partial B}{\partial z}}_{\text{buoyancy pressure perturbation}}$$

p_D **p_B**

Dynamic and buoyancy pressure perturbations

$$p' \propto \underbrace{\underbrace{e_{ij}^2}_{\text{splat}} - \underbrace{\frac{1}{2}|\boldsymbol{\omega}|^2}_{\text{spin}}}_{\text{dynamic pressure perturbation}} \quad \underbrace{-\frac{\partial B}{\partial z}}_{\text{buoyancy pressure perturbation}}$$

p_D **p_B**

- Convergence, divergence, deformation associated with **high** pressure ('splat' term)
- Rotation (of any sense) is associated with **low** pressure ('spin' term)
- **Low (high)** pressure is found **below (above)** the level of maximum buoyancy (buoyancy pressure term)

Dynamic and buoyancy pressure perturbations

$$p' \propto \underbrace{\underbrace{e_{ij}^2}_{\text{splat}} - \frac{1}{2}|\boldsymbol{\omega}|^2}_{\text{dynamic pressure perturbation}} \quad \underbrace{-\frac{\partial B}{\partial z}}_{\text{buoyancy pressure perturbation}}$$

\mathbf{p}_D **\mathbf{p}_B**

- Non-hydrostatic pressure perturbation \mathbf{p}_{NH} encompasses *ALL* of \mathbf{p}_D plus *part* of \mathbf{p}_B
- Hydrostatic pressure perturbation \mathbf{p}_H encompasses remainder of \mathbf{p}_B

$$p' = p'_{nh} + p'_h$$

$p'_d + \text{part of } p'_b$

\uparrow

p'_{nh}

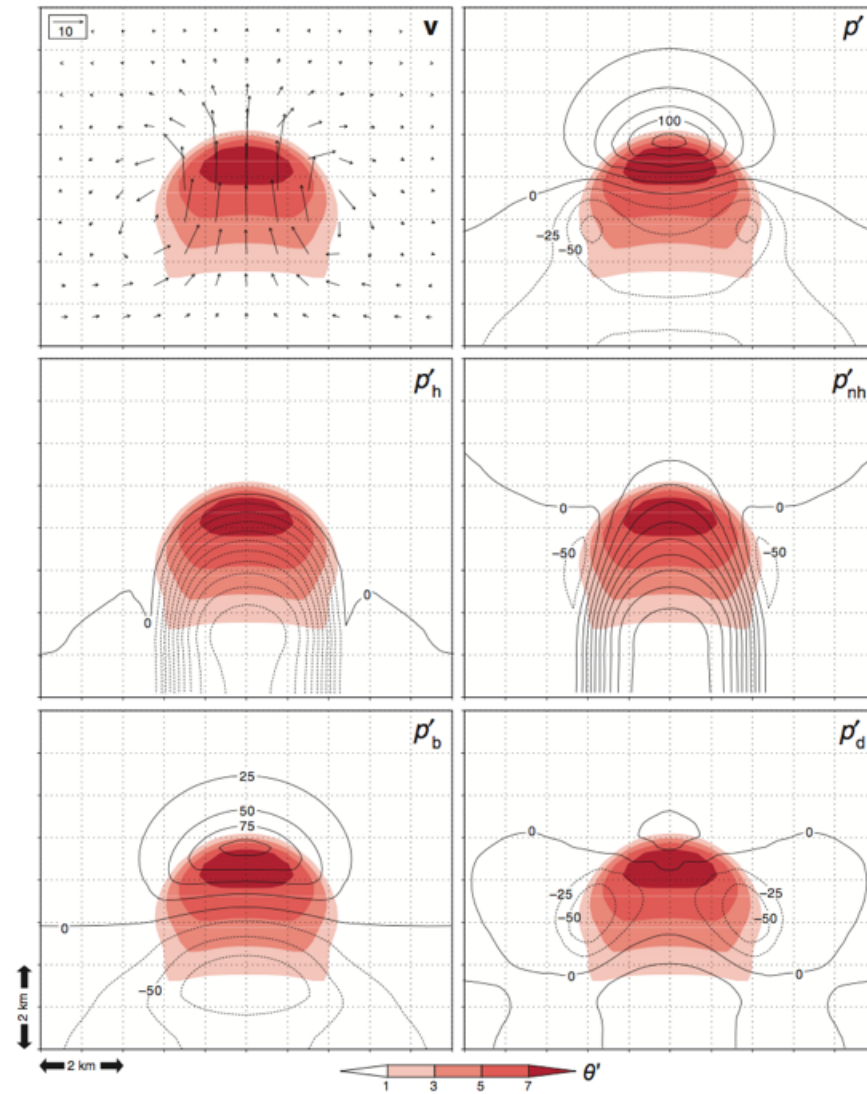
$+$

$\text{remainder of } p'_b$

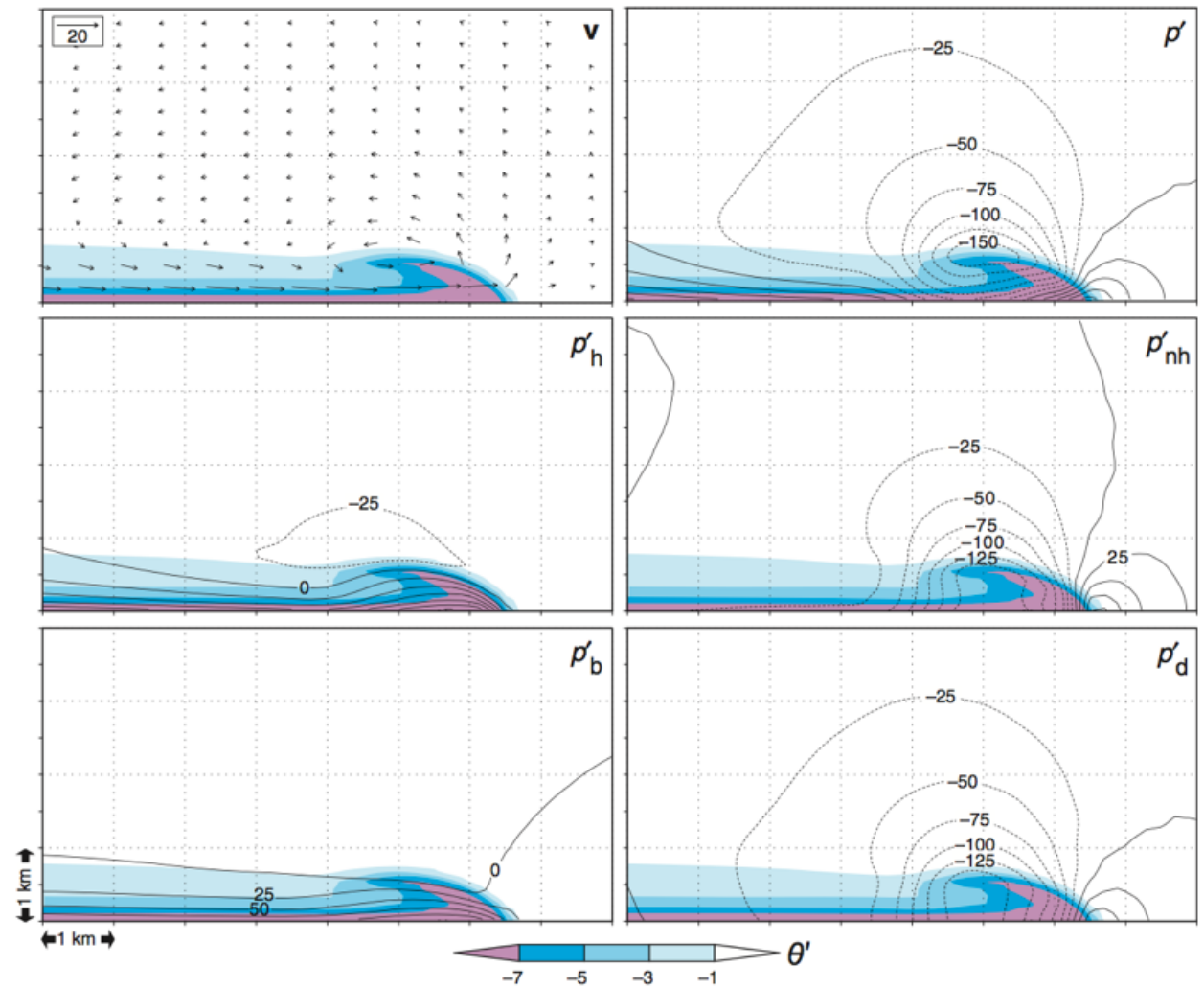
\leftarrow

p'_h

***Pressure perturbation decomposition
associated with positively buoyant bubble***



***Pressure perturbation decomposition
associated with density current***



Vertical buoyant accelerations shouldn't depend on the "environment" or "base-state", only the full field (i.e., ρ and not $\bar{\rho}$).

$$\begin{aligned}
 \frac{dw}{dt} &= -\frac{1}{\rho} \frac{\partial p'}{\partial z} + \frac{\rho'}{\rho} g = VPPGF + B \\
 \frac{dw}{dt} &= -\frac{1}{\rho} \left(\frac{\partial p'_b}{\partial z} + \frac{\partial p'_d}{\partial z} \right) + B \\
 &= \underbrace{-\frac{1}{\rho} \frac{\partial p'_d}{\partial z}}_i + \underbrace{\left(-\frac{1}{\rho} \frac{\partial p'_b}{\partial z} + B \right)}_{ii}
 \end{aligned}$$

thermal buoyancy
 D&M04 Eqn. 9

dynamic forcing *buoyancy forcing*

Term *i* is a function of the flow field – independent of the "base-state" assumed for buoyancy

Term *ii* combines "thermal buoyancy", **B**, with the buoyant contribution to the VPPGF. Thermal buoyancy increase offset by buoyant perturbation pressure gradient increase (in opposite direction).

The sum of the terms in *ii* *does not depend on the base-state*, but its partitioning does.

Dynamic and buoyancy pressure perturbations

Contributions to updraft accelerations from $\mathbf{p_D}$ can be larger than $\mathbf{p_B}$ in certain environments (e.g., those supportive of supercells).

Need to understand impacts of vertical wind shear on convection, since wind shear can lead to increases in deformation and rotation terms in diagnostic pressure equation, leading to $\mathbf{p_D}$.

Vertical wind shear

Hodograph plots **wind speed** and **direction** of wind with height of **environment**.

Connect “tips” of wind vectors at each height.

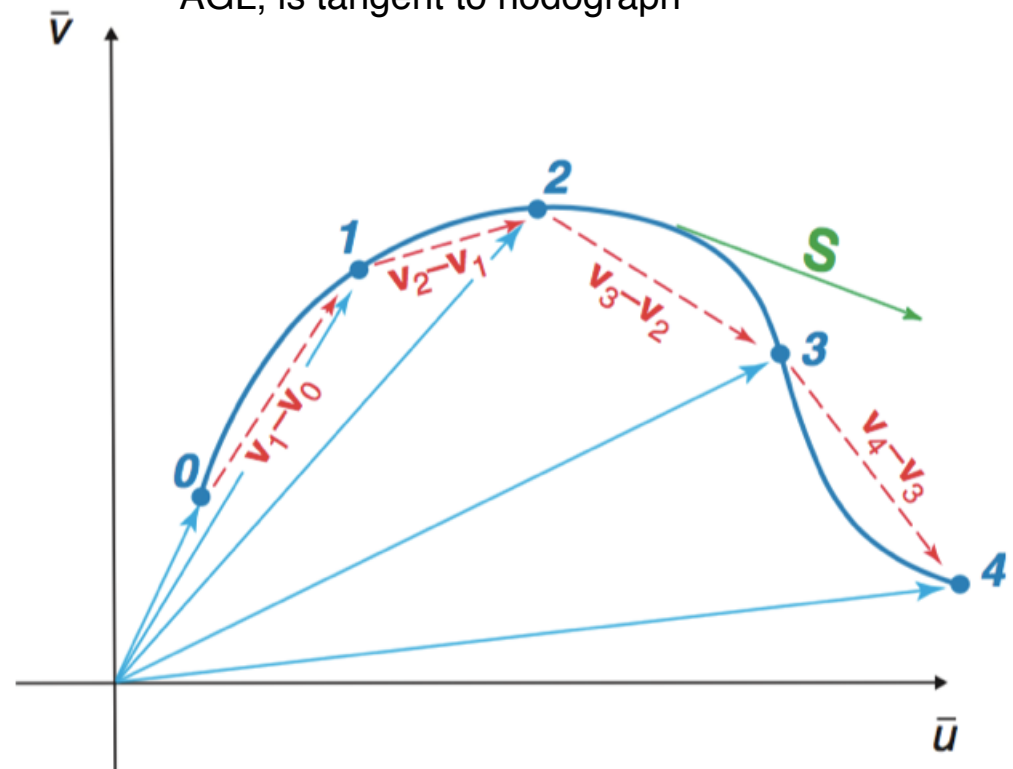
Provides information about vertical wind shear.

Long hodographs imply large vertical wind shear *magnitude*. Curvature provides information about how vertical wind shear changes with height.

Backing – counterclockwise turning with hgt

Veering - clockwise turning with hgt

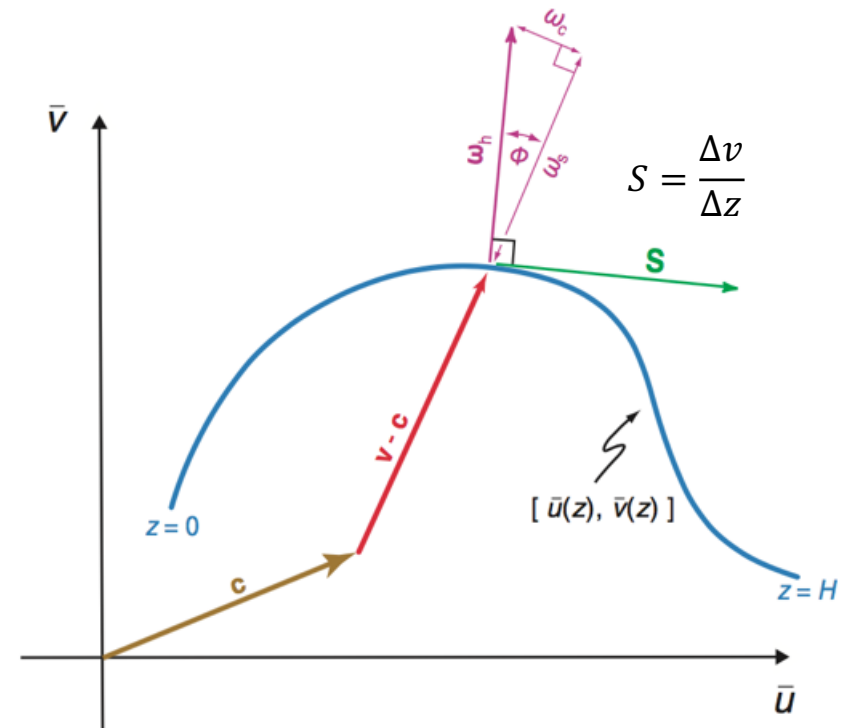
Blue vectors – wind vector at sfc, 1, 2, 3, 4 km AGL
Red vectors – wind vector difference between levels
Green vector – shear vector at a point between 2-3 km AGL, is tangent to hodograph



Vertical wind shear

Vertical wind shear vector, \mathbf{S} , related to horizontal vorticity:

$$\begin{aligned}\boldsymbol{\omega} &= \nabla \times \mathbf{v} = \begin{vmatrix} \mathbf{i} & \mathbf{j} & \mathbf{k} \\ \frac{\partial}{\partial x} & \frac{\partial}{\partial y} & \frac{\partial}{\partial z} \\ u & v & w \end{vmatrix} \\ &= \left(\frac{\partial w}{\partial y} - \frac{\partial v}{\partial z} \right) \mathbf{i} + \left(\frac{\partial u}{\partial z} - \frac{\partial w}{\partial x} \right) \mathbf{j} \\ &\quad + \left(\frac{\partial v}{\partial x} - \frac{\partial u}{\partial y} \right) \mathbf{k} \\ &= \xi \mathbf{i} + \eta \mathbf{j} + \zeta \mathbf{k}\end{aligned}$$



If horizontal gradients of \mathbf{w} small relative to vertical shear, horizontal vorticity can be written as,

$$\omega_h \approx \left(-\frac{\partial v}{\partial z}, \frac{\partial u}{\partial z} \right) = \mathbf{k} \times \mathbf{S} \quad \omega_h \text{ has same magnitude as } \mathbf{S}, \text{ pointed } 90^\circ \text{ to left of } \mathbf{S}.$$

Vertical wind shear

Can estimate *mean wind velocity* within a layer using hodograph.

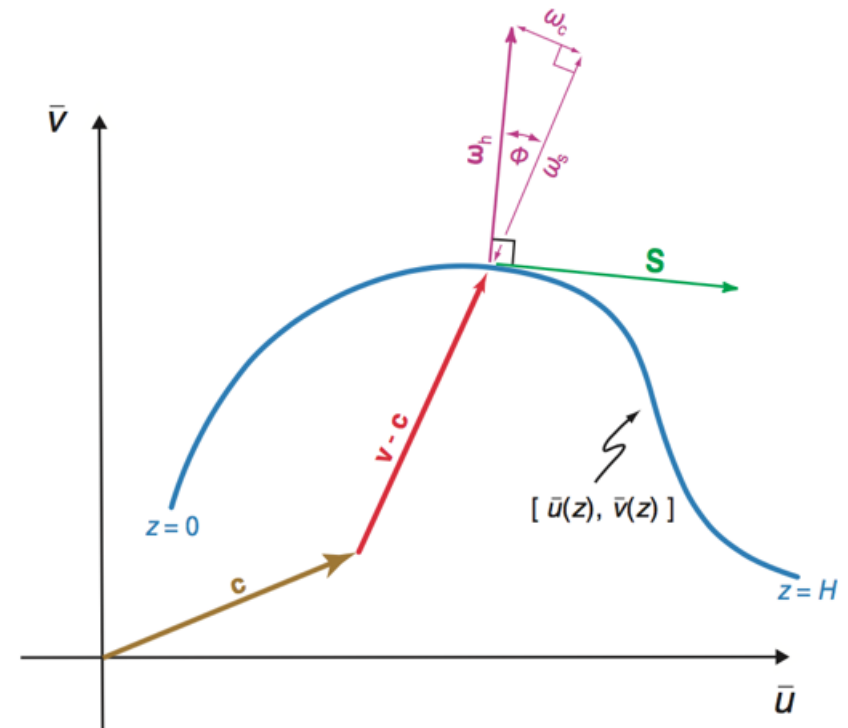
If hodograph is **straight**, mean wind velocity will **lie on the hodograph** within that layer.

If hodograph is **curved**, mean wind velocity will **lie on concave side of hodograph**.

Why is mean wind important?

Convection tends to move approximately with the mean wind velocity averaged over the depth of the storm (during early stages of lifecycle).

Later in lifecycle, *propagation* may cause storm motion that deviates from mean wind vector.



Storm motion and hodographs

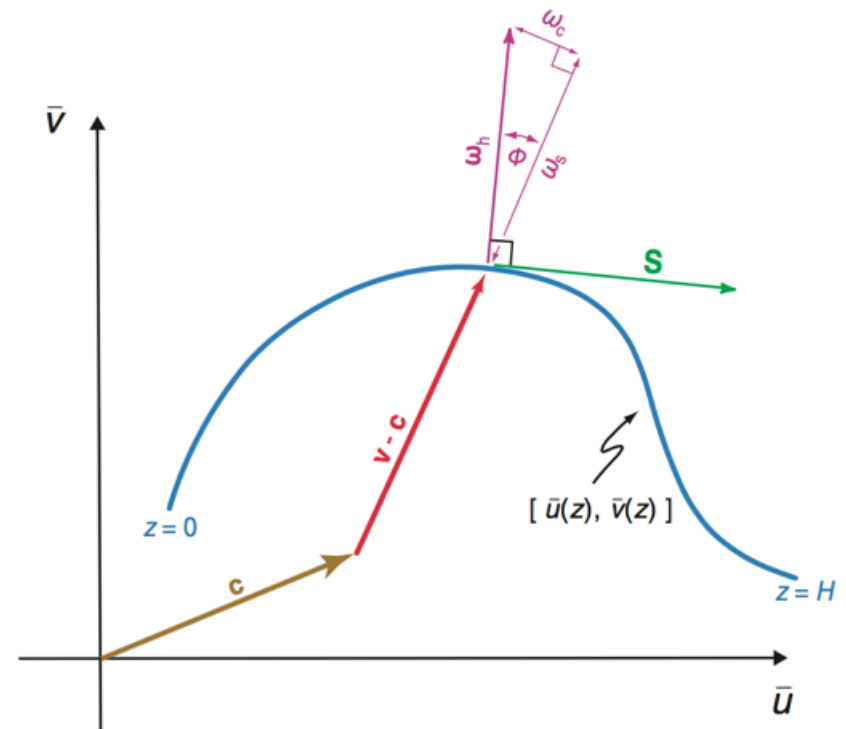
Assume \mathbf{c} in figure on right is **storm motion vector**

\mathbf{c} = advection (mean wind) + propagation

In a “storm-relative” reference frame, the wind vector at a particular height will be $\mathbf{v} - \mathbf{c}$.

Move origin of hodograph to storm motion location to get storm-relative winds. Hodograph is “Galilean invariant” when adjusted with *constant* storm motion.

Storm motion usually not exactly known a priori, estimated with hodograph or empirical techniques.



Storm motion and hodographs

Directional shear – variations in ground-relative wind direction with height.

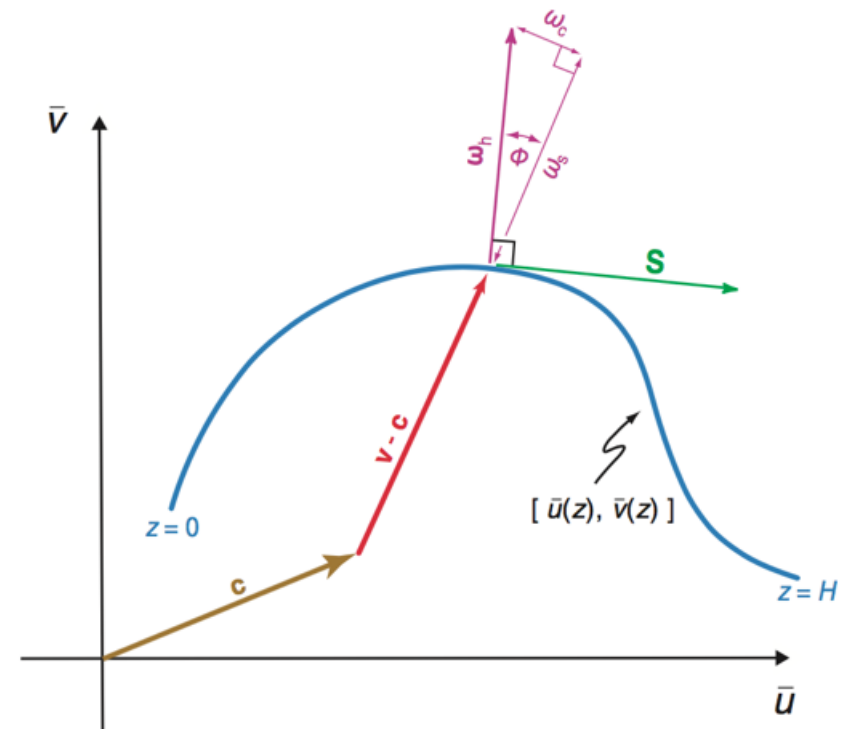
Sometimes *directional shear* refers to change in shear vector, \mathbf{S} , with height.

Unidirectional shear – straight hodograph

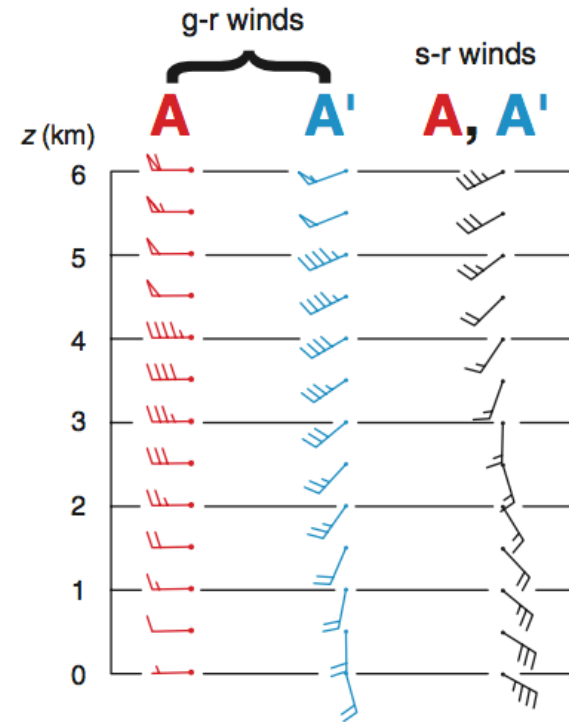
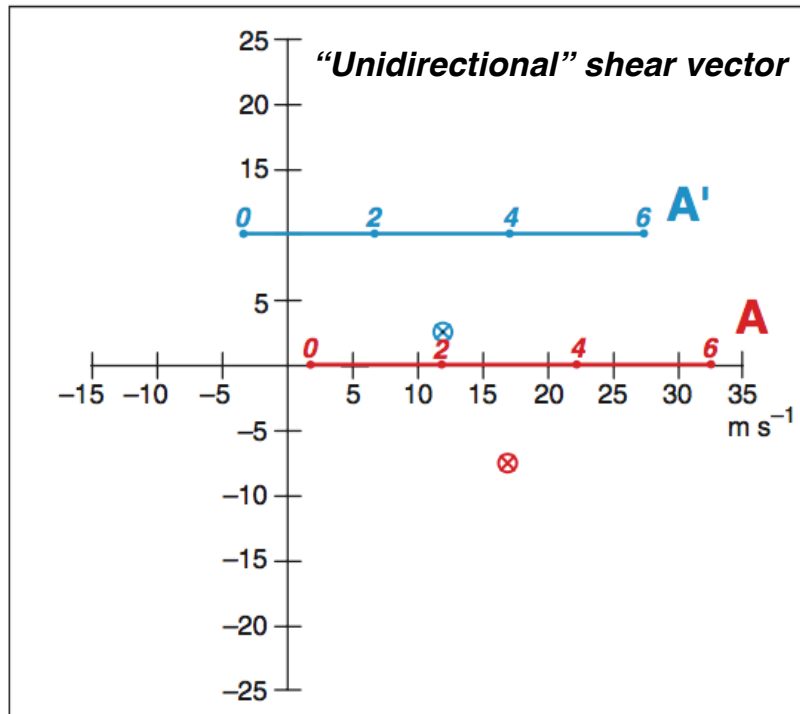
Directionally-varying shear – curved hodograph

Speed shear – variations in ground-relative wind speed with height.

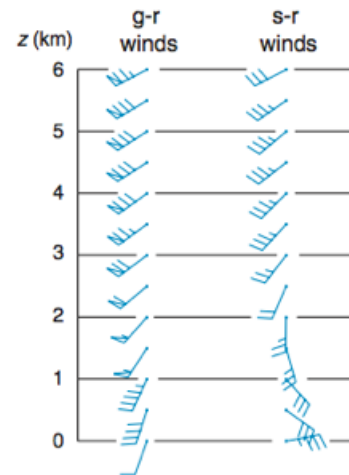
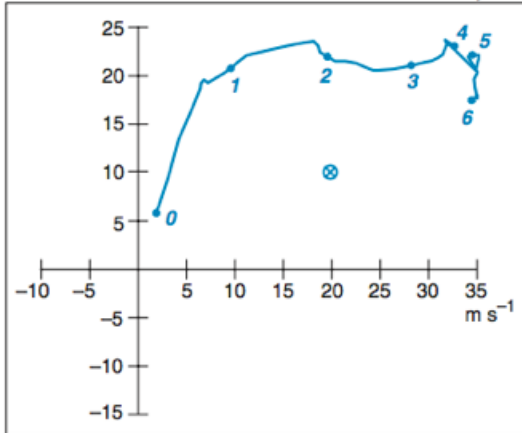
Shape and length of hodograph, and thus profiles of wind shear and s-r winds, are more dynamically relevant than vertical profile of ground-relative winds.



Moving hodograph can change g-r winds, changing g-r speed/directional shear. But s-r shear remains constant!



(a) 0000 UTC 28 March 1994 Athens, GA

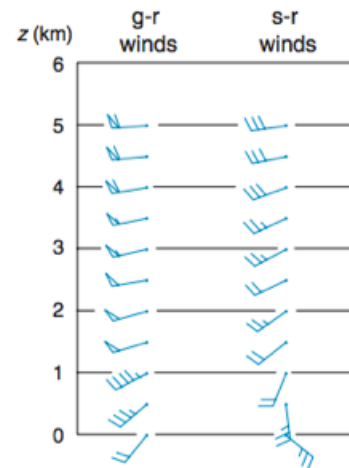
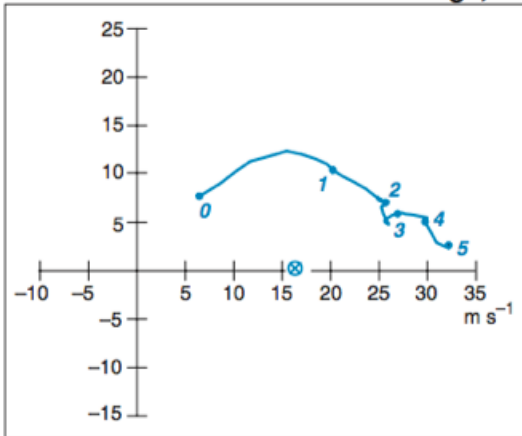


Ground-relative winds determine mean wind orientation and where hodograph is positioned relative to origin.

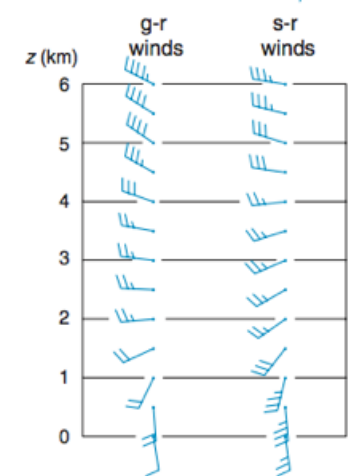
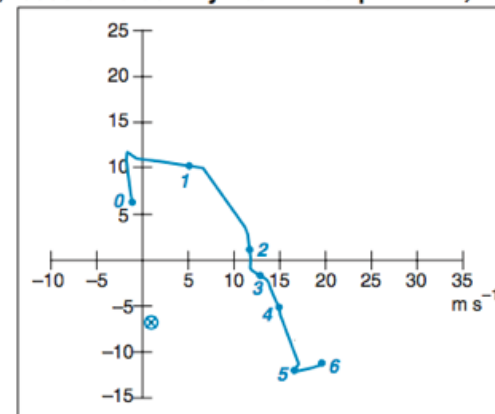
Among these three cases, mean winds are very different, but hodograph shapes are similar.

Small ground-relative veering can be associated with large storm-relative veering (e.g. panel a).

(b) 0000 UTC 1 June 1985 Pittsburgh, PA



(c) 0000 UTC 30 May 1994 Stephenville, TX



Oklahoma 2013 Tornado Outbreak Skew-T

Real hodographs are often messy....

NOAA/NWS Storm Prediction Center
Norman, Oklahoma

